Experimental Study on Oscillating Feedback Micromixer for Miscible Liquids Using the Coanda Effect

Cong Xu and Yifeng Chu
Division of Nuclear Chemistry and Chemical Engineering, Institute of Nuclear and New Energy Technology, Tsinghua University, Beijing 100084, P.R. China

DOI 10.1002/aic.14702
Published online December 11, 2014 in Wiley Online Library (wileyonlinelibrary.com)

An oscillating feedback micromixer with no moving parts comprises an inlet channel, a diverging mixing chamber, a splitter, two feedback channels, and an outlet channel. Using the Coanda effect, two liquids are passively mixed in an oscillating feedback micromixer. Three oscillating feedback micromixers were experimentally investigated using two miscible liquids. The first had asymmetric feedback channels and a splitter, the second had symmetric feedback channels and a splitter, and the third had symmetric feedback channels and no splitter. Three chaotic mixing modes—vortex mixing, internal recirculation mixing, and oscillating mixing—were observed with increasing Reynolds numbers. The asymmetric oscillating feedback micromixer was determined to have the best mixing performance among the three micromixers. The splitter and asymmetric feedback channels can facilitate internal recirculation through feedback channels and fluidic oscillation, thereby enhancing the mixing efficiency. A completed mixing was achieved in the asymmetric micromixer. © 2014 American Institute of Chemical Engineers *AIChE J*, 61: 1054–1063, 2015
Keywords: passive micromixer, Coanda effect, vortex, internal recirculation, oscillation

Introduction

In the past decade, micromixers have found comprehensive applications in micrototal analysis systems and microreactors.[1,2] Micromixers can be classified as active micromixers or passive micromixers according to the presence of an external energy supply. In active micromixers, mixing is completed by supplying external energy from sources such as ultrasound, acoustically induced vibrations, electrokinetic instabilities, and small impellers. In contrast, passive micromixers enhance mixing efficiency using hydrodynamic forces generated in specially designed microchannel configurations, without any external energy input. Furthermore, passive micromixers have no moving parts. Thus, passive micromixers can be fabricated and controlled easily. In contrast to passive micromixers, active micromixers have generally moving parts and/or complicated control systems and input systems for supplying external energy. The fabrication of moving parts inside an active micromixer is considerably difficult. Control systems and energy input systems generally have much larger volume than micromixers. Hence, it is difficult to integrate these two systems and an active micromixer. Thus, passive micromixers exhibit greater potential for efficient use than active micromixers.

According to the flow patterns in microchannels, passive micromixers can be roughly classified into three: lamination, droplet, and chaotic advection micromixers. Because of the micromixers' small dimensions, flows in all three types of passive micromixers are laminar. In lamination micromixers, two or more lamellae are formed in microchannels, in which no transverse flow occurs. Mass transfer between two adjacent lamellae is dominated by molecular diffusion. To enhance mixing efficiency, reducing mixing path is essential for lamination micromixers. Thus, generating lamellae as thin as possible is essential in channel design for lamination micromixers. The inlet configuration is an important factor affecting lamellae's thickness. Lamination micromixers can be classified as T-type micromixers,[3,4] Y-type micromixers,[5] or hydraulic focusing micromixers[6,7] according to their inlet configurations. A split and recombine flow micromixer can be roughly considered as a cascade of multiple lamination micromixers.[8,9] In a T-type or Y-type micromixer, mixing can be improved when an asymmetric two vortex flow regime, identified from the planar topology in the T-channel junction and denoted engulfment flow, occurs at moderate Reynolds numbers.[10–12] However, in most of the lamination micromixers, because the diffusion rate caused by the thermal motion of molecules is low, a long mixing channel is typically required to ensure sufficient mixing time. In droplet micromixers, two different liquids are fed into a microchannel through a T-type inlet or coaxial inlet. Because of surface tension, droplets are formed in the microchannel, and the required mixing path is reduced.[13–16] To ensure the formation of droplets, the flow rates of liquids, that is, the Reynolds numbers, should be sufficiently low. In contrast with lamination and droplet micromixers, chaotic advection micromixers generate secondary recirculating flows with transverse velocity components that are perpendicular to the axial direction of microchannels. Because of the secondary recirculating flows, periodical fluctuations of the flow field generate along the axial direction of the microchannels, and the chaotic advection mixing occurs.[17,18] In a chaotic

Correspondence concerning this article should be addressed to C. Xu at c-xu@mail.tsinghua.edu.cn.

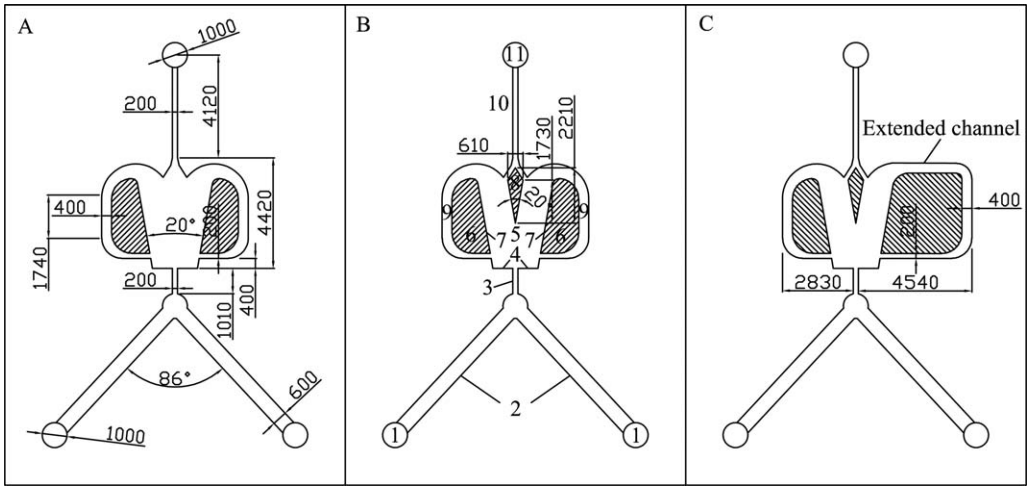

Figure 1. Configurations and dimensions of oscillating feedback micromixers (Unit: micrometer).

(1) Inlet port; (2) Y-feed channel; (3) inlet channel; (4) Coanda step; (5) mixing chamber; (6) barrier; (7) attachment wall; (8) splitter; (9) feedback channel; (10) outlet channel; and (11) outlet port.

advection mixing, the transverse velocity components destroy regular lamination flows to form transverse flows, in which microfluidic lumps are split, stretched, folded, or broken up.[1,19–27] Consequently, the interfacial area is greatly increased, and the required mixing length is reduced. Because the interfacial area can increase exponentially and be operated at high Reynolds numbers, chaotic advection micromixers have more potential applications than lamination and droplet micromixers. Generating secondary recirculating flow is a key in the design of chaotic advection micromixers. A number of specially designed channel configurations have been proposed to induce secondary recirculating flow. The reported specially designed channels can be roughly classified as two-dimensional (2-D) structures or 3-D structures. Two typical designs are used for 2-D structures. No linear mixing channels, such as alternating curved channels, zigzag channels, and square wave channels, were designed to generate secondary recirculating flows and achieve transverse dispersion.[20,28–30] Hong et al.[21] proposed an inplane passive microfluidic mixer with Tesla structures. The Tesla structures can produce Poisseuille flow transverse to the main flow, and the collision caused by the Coanda effect results in intense transverse dispersion. However, most of the microchannels used to produce chaotic flow are complicated 3-D structures. A staggered herringbone arrangement of ridges or grooves on the wall of a mixing channel was proposed and investigated to induce transverse flows.[19,31] Kim et al.[24] developed barrier embedded micromixers in which a complicated Kenics structure was used to induce chaotic flow. Twisted microchannels such as wavelike channels were used to induce a chaotic mixing effect.[32] However, to date, the fabrication of microchannel configurations used to produce secondary recirculating flow has been complicated, limiting the applications of chaotic advection micromixers.

In this article, 2-D passive oscillating feedback micromixers were designed using the Coanda effect and experimentally investigated. The micromixers have a simple configuration and are easily fabricated. Efficient chaotic advection mixing of two miscible liquids can be achieved in the micromixers using vortex mixing, internal recirculation, and oscillation.

Experimental

Oscillating feedback micromixer

The oscillating feedback micromixers that were investigated were designed to make use of the Coanda effect. The Coanda effect is a wall-attachment flow phenomenon that generally occurs when a fluid flows at high speed from a narrow passage into a suddenly enlarged chamber with two side walls.[33] The fluid entering into the chamber can entrain the surrounding fluid. Because some of the fluid molecules between the inlet fluid and each side wall are evacuated, a low-pressure region is formed on both sides of the inlet fluid, causing a counterflow down each side wall. Generally, the inlet fluid cannot flow straight through the enlarged chamber. Any perturbation (e.g., a turbulent fluctuation) may bend the inlet fluid toward one side wall, cutting down the counterflow and lowering the pressure in the low-pressure region near that side wall. This mechanism causes the inlet fluid to attach to that side wall. In 1970s, Tippetts et al.[34] investigated fluidic oscillators with a control loop using the Coanda effect. They found that a periodically oscillating flow at a fixed frequency is generated by the Coanda effect in the enlarged chamber, and the frequency is proportional to the flow rate. Another fluidic oscillator called the fluidic feedback oscillator has also been designed, using two feedback channels to replace the control loop.[35] The fluidic feedback oscillator can generate an oscillating feedback flow with a fixed frequency that is proportional to the flow rate in the enlarged chamber, using the Coanda effect. This phenomenon of an oscillating feedback flow has been used in flow measurement and extraction.[36–38] When two liquids are fed into an enlarged chamber at a high velocity, the oscillation can destroy regular parallel flows and effectively mix the two liquids. The key challenge in using the Coanda effect in mixing is designing a special microchannel to generate oscillation.

Three oscillating feedback micromixers were designed and fabricated in this study. As shown in Figure 1, an oscillating feedback micromixer comprises an inlet channel, a divergent mixing chamber, two feedback channels, and an outlet channel. A Y-type feed channel is connected to the inlet channel. The width of the mixing chamber entrance is larger than the

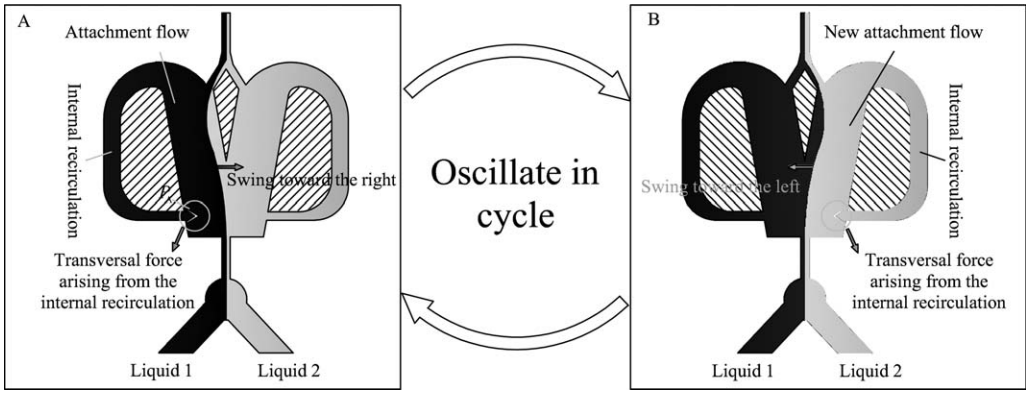

Figure 2. Schematic of mixing mechanism in oscillating feedback micromixers (complicated transverse flows between two liquids is not demonstrated).

width of the inlet channel, forming two Coanda steps. Two feedback channels are recirculated near the exit of the inlet channel from the junction between the mixing chamber and the outlet channel. The three micromixers are different. The micromixer shown in Figure 1A has symmetric feedback channels and no splitter. Except for the splitter, all dimensions of the micromixer shown in Figure 1B are identical to those of Figure 1A. In contrast with Figures 1A, B, the right feedback channel of the micromixer shown in Figure 1C is extended, and thus, the feedback channels are asymmetric. The same splitter as that in Figure 1B is placed inside the micromixer shown in Figure 1C, and all dimensions, except for the dimensions of the extended feedback channel, are identical to those in Figures 1A, B. A micro-oscillator similar to Figure 1C was proposed by Yang et al.[39] to measure flow and accelerate a reaction between the two fluorescent proteins. However, the splitter and the comparison between the asymmetric and symmetrical channels have not been investigated. Using the micromixer shown in Figure 1B as an example, Figure 2 illustrates the Coanda effect for complete mixing. Two liquids are fed simultaneously into the suddenly enlarged mixing chamber. The liquids entering the mixing chamber are guided by the Coanda steps and tend to follow the left attachment wall (or the right attachment wall; Figure 2A). Inside the mixing chamber, the pressure P_B near the entrance of the outlet channel is larger than P_A near the exit of the inlet channel because the mixing chamber is enlarged downstream. Because of the pressure differential between the two ends of the left feedback channel, internal recirculation is formed through the feedback channel. At the port of the left feedback channel near the exit of the inlet channel, the recirculating flow exerts a transverse force on the wall-attachment flow along the left attachment wall. Consequently, the wall-attachment flow shifts toward the right. The right Coanda step causes this flow to form a new wall-attachment flow along the right attachment wall (Figure 2B). Similarly, the recirculating flow through the right feedback channel pushes the wall-attachment flow away from the right attachment wall and returns it to the left attachment wall. Thus, the flows of two liquids oscillate inside the micromixer. During this fluidic oscillation, the transverse force can effectively destroy regular parallel flows and form transverse flows. Consequently, liquid lumps are split, stretched, folded, and broken up, and efficient chaotic advection mixing is expected in oscillating feedback micromixers.

The configurations and dimensions of the three oscillating feedback micromixers used in this study are shown in Figure 1. The depth of each of these micromixers is 1000 μm. All micromixers were machined using a precision machine tool in an 8-mm thick transparent poly methyl methacrylate (PMMA) plate. The transparent PMMA material enables the visualization of the flow patterns in the micromixers. A smooth PMMA plate 6 mm thick was fixed to the slotted PMMA plate using a clamp. The clamped PMMA plates were immersed in an absolute alcohol solution and maintained at 40°C inside an ultrasound oscillator for 25 min. Then, the two PMMA plates were firmly bonded to form a complete oscillating feedback micromixer. After being cleaned using deionized water, the micromixer was used to evaluate mixing performance for two miscible liquids.

Materials and experimental setup

Colorless deionized water and a dark-blue aqueous solution were used as the two liquids to be mixed. All mixing experiments were performed at 14–15°C. The dark-blue aqueous solution was prepared by adding 1 g of blue dye (Brilliant Blue FCF, Clariant International, Switzerland) to 300 g of deionized water. The density and viscosity were 999 kg m^{-3} and 1.16×10^{-3} Pa s, respectively, for the colorless water and 1001 kg m^{-3} and 1.44×10^{-3} Pa s, respectively, for the dark-blue aqueous solution. The densities and viscosities were measured using a density meter (Den Di-1, Beijing YILUDA Co., Beijing, P.R. China) and a rotary viscosimeter (DV-1, Spain Fungilab Company, Barcelona, Spain). When the dark-blue aqueous solution diffused into the colorless water, the resulting mixture appeared light blue.

The experimental flowchart is shown in Figure 3. Two precise syringe pumps (Baoding Longer Precision Pump Co., LSP01-1BH, stroke resolution: 0.156 μm) were used to simultaneously pump the colorless and dark-blue liquids into the inlet ports. The volume rate ratio of the two liquids was maintained at 1:1 throughout all tests. A halogen lamp was used as the light source. The light emitted from the lamp passed through an oscillating feedback micromixer. Some light was absorbed by the blue dye molecules within the micromixer, resulting in a reduction of the transmitted light intensity. The reduction of the light intensity is dependent on the concentration of the blue dye. A microscope (Shanghai Changfang Optical Instrument Factory, CMM-50E) was placed above the micromixer to visualize the flow patterns in

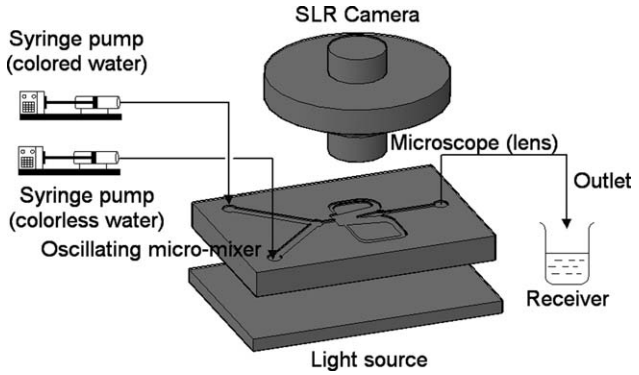

Figure 3. Experimental flowchart.

the micromixers. A digital single lens reflex (SLR) camera (Canon, EOS650D, 5184 × 3456 pixels) was installed on the microscope to sense the transmitted light and record the images of flow patterns.

Results and Discussions

Mixing mechanisms

The three oscillating feedback micromixers shown in Figure 1 were all investigated experimentally. Three mixing mechanisms were observed with increasing Reynolds numbers. The flow patterns in the micromixer with asymmetric feedback channels and a splitter (Figure 1C) are used to demonstrate the three mechanisms because this micromixer's mechanisms are the most obvious among the three micromixers. The Reynolds number, *Re*, is defined as follows

$$Re = \frac{\rho U d}{\mu} \tag{1}$$

where ρ and μ are the density and viscosity, respectively, of the dark-blue aqueous solution. U is the apparent velocity of the dark-blue solution (or the colorless deionized water) at the exit of the inlet channel, and d is the hydrodynamic diameter of the exit of the inlet channel.

Vortex Mixing. As shown in Figure 4A ($Re = 38.6$), both the dark-blue and colorless liquids enter the mixing chamber in parallel through the inlet channel, and a distinct boundary dividing the two laminar flows can be observed inside the inlet channel. The left side of the mixing chamber and the left feedback channel are filled with the dark-blue liquid. The dark-blue flow is split at the tip of the splitter and intrudes into the right side of the mixing chamber. The split dark-blue flow becomes light blue because of dilution, and it flows around the splitter and then enters the outlet channel. Because the mixing chamber is diverging, the downstream pressure P_B is larger than the upstream pressure P_A. Two clockwise recirculating flows light blue in color, that is, the outer vortex and the inner vortex, can be observed in the right side of the mixing chamber. An obvious vortex center can also be seen. The vortices are produced by the pressure difference between P_B and P_A and the shear force caused by the forward flow near the center line of the mixing chamber. The light-blue liquid can be used to trace the flow of the colorless water in the right side of the mixing chamber. No liquid is recirculated through the right feedback channel because the difference between P_B and P_A is not sufficiently large to overcome the resistance of the flow through the feedback channel. Furthermore, no oscillation was observed during the test. Figure 4B demonstrates the flow pattern with *Re* increased to 57.9. This flow pattern is similar to that in Figure 4A, but the color of the light-blue liquid in the right side of the mixing chamber is darker than that in Figure 4A. Even with an *Re* of 57.9, the mixing is inefficient because the color is not uniform inside the mixing chamber and the outlet channel. In conclusion, at low Reynolds numbers, neither internal recirculation through the feedback channels nor oscillation occurs. Although increasing *Re* can improve mixing performance, efficient mixing cannot be achieved by simply using the vortices inside the mixing chamber.

Internal Recirculation Mixing. Figure 4C shows the flow pattern with *Re* increased to 77.2. It is obvious that a light recirculation is formed through the right feedback channel. The light-blue recirculating liquid flows along the inner side of the channel and does not fill the channel. When *Re* is further increased to 81.1 (Figure 4D), the right feedback channel is filled with the light-blue recirculating liquid, and the right side of the mixing chamber is occupied by a light-blue vortex. The mixing performance is substantially enhanced compared to that in Figures 4A, B. During the tests, the oscillation was not obvious. The mixing between the two liquids is mainly dependent on the vortex mixing inside the mixing chamber and the internal recirculation through the feedback channels.

Oscillation Mixing. The photographs in Figures 4E–H were taken at intervals of 0.2 s at an *Re* of 96.5. As shown in these figures, the distinct boundary between the left dark-blue flow and the colorless flow can clearly be seen. In Figure 4E, the boundary on the right deviates from the center line and is shifting toward the left. The boundary on the right means that the main flow direction deflects to the right. This indicates that due to the Coanda effect, an attachment flow is formed on the right attachment wall; at 0.2 s, the boundary reaches the center line of the mixing chamber (Figure 4F); at 0.4 s, the boundary moves to the left of the mixing chamber (Figure 4G). Similar to Figure 4E, the boundary on the left means that an attachment flow is formed on the left attachment wall (Coanda effect); at 0.6 s, the boundary has shifted back to the right (Figure 4H). Namely, when *Re* is increased to 96.5, the main flow direction of the liquids in the mixing chamber periodically deflects to the right and the left. The periodical deflection of the main flow direction is known as "oscillation."[36,37] It should be noted that the mixing performance in Figures 4E–H is greatly improved compared with Figures 4A–D. Increasing Reynolds numbers can effectively enhance the mixing performance. Figure 4I demonstrates the mixing at an *Re* of 386.1, in which the color is nearly uniform in the left and right sides of the mixing chamber and in the outlet channel. Thus, efficient and uniform mixing can be achieved using the oscillating feedback micromixer with high Reynolds numbers. During the oscillation, the internal recirculation and the vortex inside the mixing chamber are intense. Because the two miscible liquids are almost uniformly mixed, the vortex flows are not apparent in Figures 4E–I. It should be noted that the oscillation cannot occur unless the Reynolds number, that is, the flow rate of the liquids at the exit of the inlet channel, is sufficiently large. This is because the sufficiently large flow rate is necessary for the Coanda effect.

In conclusion, three mixing mechanisms, that is, vortex mixing, internal recirculation mixing, and oscillation mixing, occur successively in an oscillating feedback micromixer

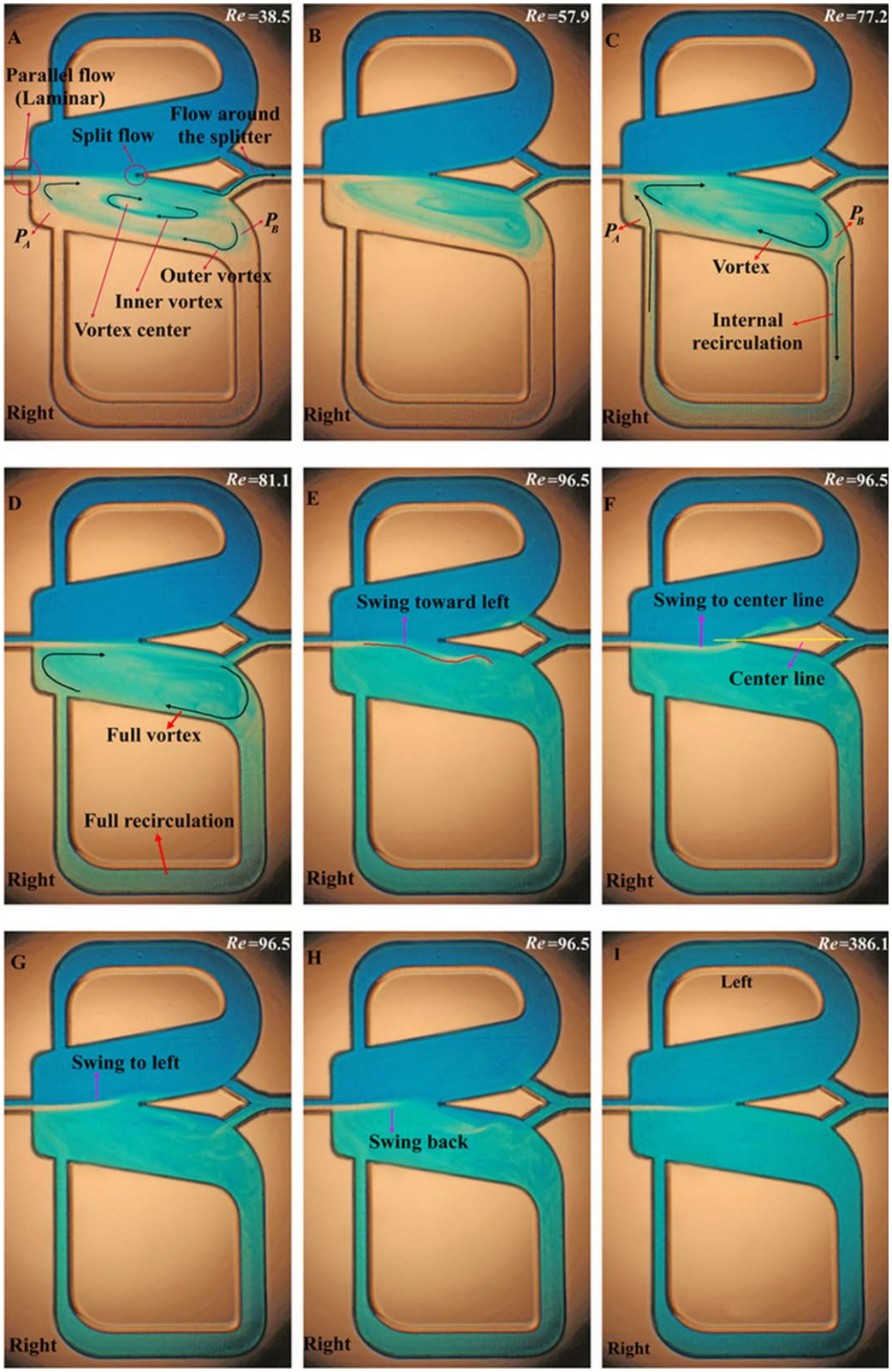

Figure 4. Flow patterns inside an oscillating feedback micromixer with asymmetric feedback channels and a splitter: (A) $Re = 38.5$; (B) $Re = 57.9$; (C) $Re = 77.2$; (D) $Re = 81.1$; (E) $Re = 96.5$, $t = 0$ s; (F) $Re = 96.5$, $t = 0.2$ s; (G) $Re = 96.5$, $t = 0.4$ s; (H) $Re = 96.5$, $t = 0.6$ s; and (I) $Re = 386.1$.

[Color figure can be viewed in the online issue, which is available at wileyonlinelibrary.com.]

with increasing Reynolds numbers. The three mixing mechanisms enable the transverse movement of liquid lumps inside laminar parallel flows. Consequently, efficient chaotic advection mixing can be achieved. When oscillation occurs, two miscible liquids can be effectively mixed, and each of the three mixing mechanisms play an important role.

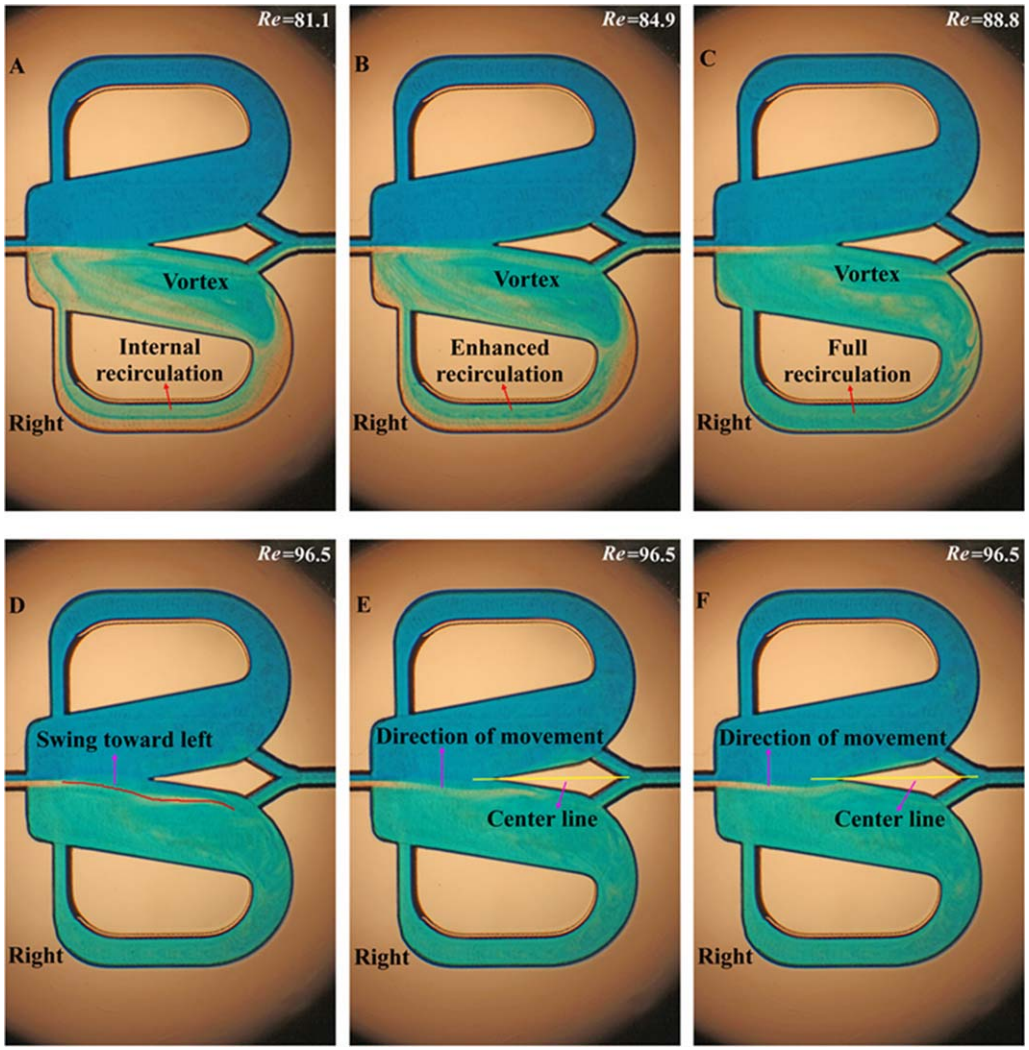

Figure 5. Flow patterns inside an oscillating feedback micromixer with symmetric feedback channels and a splitter: (A) $Re = 81.1$; (B) $Re = 84.9$; (C) $Re = 88.8$; (D) $Re = 96.5$, $t = 0$ s; (E) $Re = 96.5$, $t = 0.2$ s; and (F) $Re = 96.5$, $t = 0.4$ s.

[Color figure can be viewed in the online issue, which is available at wileyonlinelibrary.com.]

Effects of symmetry of the feedback channels

As previously mentioned, the secondary recirculating flow with transverse velocity components inside laminar parallel flows is a primary factor in chaotic advection mixing. Enhancing the internal recirculation through feedback channels and oscillation is effective for improving the mixing performance of oscillating feedback micromixers. It is noted that when the transverse force acting on the left side of a flow entering the mixing chamber is equal to that acting on the right side of the flow, the flow tends to pass straight through the mixing chamber without oscillation. Unbalanced transverse forces can enhance the internal recirculation and oscillation and thereby improve the mixing performance of oscillating feedback micromixers. The micromixer with asymmetric feedback channels was designed on the basis of this idea (Figure 1C). Compared with the micromixer in Figure 1B, the right feedback channel of the micromixer in Figure 1C is extended. The extended feedback channel is longer than the left feedback channel and consequently has higher flow resistance. Thus, the recirculating flow through the shorter left feedback channel is larger than that through the longer right feedback channel. The transverse force acting on the wall-attachment flow is stronger for larger recirculating flow. Therefore, owing to the unequal recirculating flows, unbalanced transverse forces are obtained. To verify the significance of the asymmetric feedback channels, the micromixer with symmetric feedback channels was investigated. Figures 5A–F show the flow patterns inside the micromixer with symmetric feedback channels. As shown in Figures 5A–C, the right feedback channel and the right side of the mixing chamber are not filled with the light-blue liquid with an Re of 81.1 or 84.9; they are filled with the light-blue liquid only when Re reaches 88.8. In contrast, in Figure 4D, wherein Re is 81.1, the extended right feedback channel and the right side of the mixing chamber are filled with the light-blue liquid. Furthermore, for the micromixer with asymmetric feedback channels and an Re of 96.5, the boundary shifts from the right to the left at approximately 0.4 s, as shown in Figures 4E–G. However, for the micromixer with symmetric feedback channels and the same Re, the boundary does not even reach the center line after 0.4 s, as shown in Figures 5D–F. Thus, the asymmetric feedback channels can effectively enhance the

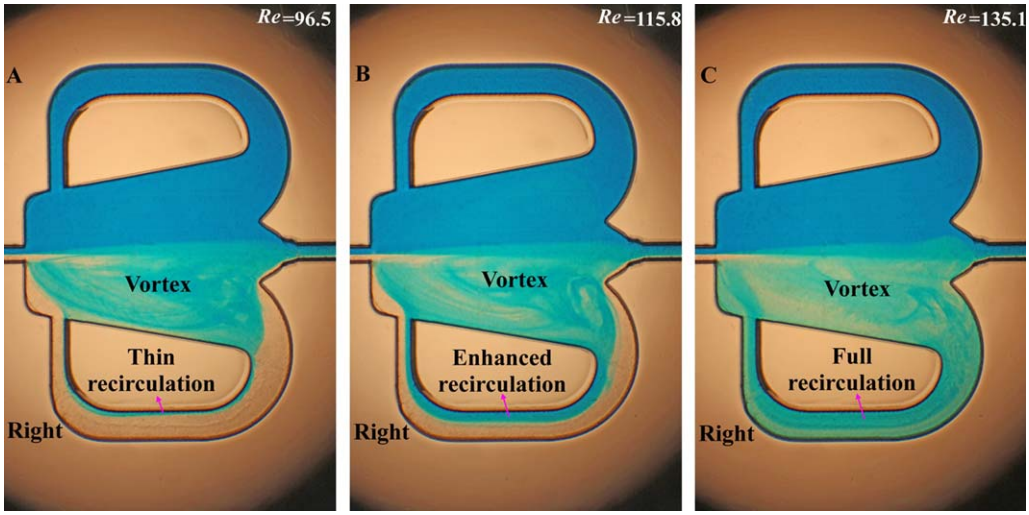

Figure 6. Flow patterns inside an oscillating feedback micromixer with symmetric feedback channels and without a splitter: (A) *Re* = 96.5, (B) *Re* = 115.8, and (C) *Re* = 135.1.

[Color figure can be viewed in the online issue, which is available at wileyonlinelibrary.com.]

internal recirculation and the oscillation, consequently enhancing the chaotic advection mixing.

Effects of splitter

Large recirculating flows through the feedback channels can enhance the transverse force and facilitate the oscillation. A splitter placed near the entrance of the outlet channel can force more liquid to enter the feedback channels. To verify the significance of the splitter, the micromixers shown in Figures 1A and B were compared. As shown in Figure 6, slight, light-blue recirculation is formed in the micromixer without the splitter until *Re* is increased to 96.5 (Figure 6A), and it is enhanced at an *Re* of 115.8 (Figure 6B). Finally, at an *Re* of 135.1, the right feedback channel and the right side of the mixing chamber are filled with the light-blue liquid (Figure 6C). In contrast to the micromixer without the splitter, a full vortex inside the right side of the mixing chamber and full recirculation through the right feedback channel are achieved at an *Re* of 88.8 (Figure 5C) in the micromixer with the splitter (Figure 1B). Furthermore, at an *Re* of 96.5, no obvious oscillation was observed in the micromixer without the splitter; at the same Reynolds number, obvious oscillation was observed in the micromixer with the splitter (Figures 5D–F). Thus, it can be proved that the splitter can enhance the internal recirculation through the feedback channels and the oscillation.

Evaluation of mixing performance

To qualify the mixing performance, the experimental images were analyzed using a digital image processing technique (MATLAB software). A blue dye was used to trace flows and mixings in all the experiments. The digital SLR camera records color images by decomposing the transmitted light into three components: red, blue, and green. When a beam of light passes through a micromixer, the blue dye molecules can completely absorb the red light component but not the blue light component. The green light component can also be absorbed by the blue dye molecules, but the extent of absorption (and therefore, the green light intensity in the transmitted light) depends on the concentration of the blue dye. Thus, the green light component that is recorded in an image can represent the distribution of the blue dye molecules within the micromixer. In the processing procedure, the captured color digital images were converted to gray scale images of the green light component, in which the gray scale levels were ranged from 0 to 255 where zero represents the lowest light intensity and 255 the highest. To eliminate the effects of the splitter and feedback channels, only the symmetric image areas shown as Figure 7 were considered. Furthermore, the origin gray scale levels (0–255) in the selected area were normalized between zero and one, using Eq. 2 to eliminate the effects of the light source, microscope, and SLR

$$I_{i,\mathrm{n}} = \frac{I_{\max} - I_i}{I_{\max} - I_{\min}} \tag{2}$$

Where I_i is the gray scale value (between 0 and 255) of pixel i when a dark-blue solution of 1-g dye/300-g water and a colorless solution (0-g dye/300-g water) are used as the two liquids that are separately fed into the micromixer. $I_{i,\mathrm{n}}$ is the normalized gray scale level for the original gray scale

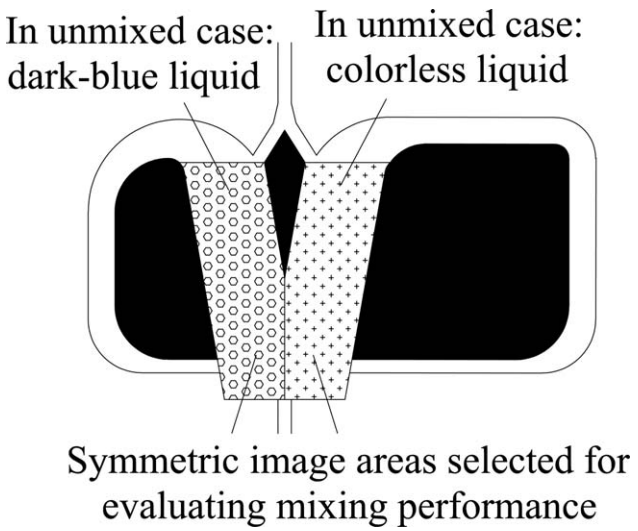

Figure 7. Selected areas used to evaluate mixing performance.

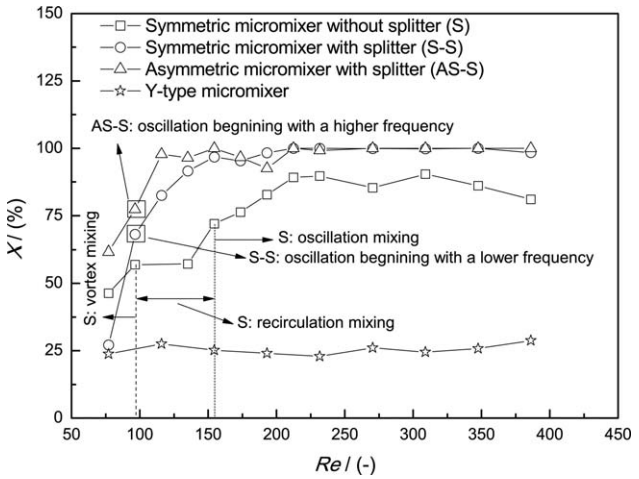

Figure 8. Comparison of mixing performance.

level I_i. I_{max} and I_{min} are the maximum gray scale level and minimum gray scale level in the selected area, respectively. The standard deviation of the light intensity distribution for the selected image area was defined as follows

$$\sigma=\sqrt{\frac{1}{N}\sum_{i=1}^{N}\left[I_{i,n}-\overline{I_{i,n}}\right]^2} \tag{3}$$

where N is the number of pixels in the selected image area, and $\overline{I_{i,n}}$ is the average value of all $I_{i,n}$ in the selected area. Furthermore, the mixing index X can be determined to characterize the mixing performance as follows

$$X=\frac{\sigma_{um}-\sigma}{\sigma_{um}-\sigma_{cm}}\times 100\% \tag{4}$$

where σ_{cm} and σ_{um} are the standard deviations for the completed mixing and no mixing, respectively. The flow rates of the dark-blue solution and the colorless water were identical in all experiments. The concentration of the perfectly mixed mixture for the two liquids, therefore, is 0.5-g dye/300-g water. To obtain σ_{cm}, a uniform solution with 0.5 g dye/300 g water was fed into the oscillating feedback micromixer and fully occupied it. Then, a color image was captured and subsequently converted to the gray scale digital image of the green light component. σ_{cm} was determined based on the gray scale digital image using Eqs. 2 and 3. No mixing is an extreme case where ideally, the dark-blue solution and colorless water occupy the left half and the right half of the micromixer, respectively, as shown in Figure 7. To obtain the standard deviation σ_{um}, only a single liquid, either the dark-blue solution or the colorless water, was fed into the oscillating feedback micromixer. One image was captured for only feeding in the single dark-blue solution, and then other was captured for only feeding in the single colorless water. Subsequently, the left half of the selected area in the image captured for only feeding in the single dark-blue solution, and the right half of one for only feeding in the single colorless water were taken out to stitch a new reference image area together. The standard deviation σ_{um} can be determined based on the new reference image area using Eqs. 2 and 3. In all the experiments, the light source intensity, distances from the light source to the micromixer and from the micromixer to the lens, and amplification factor of the microscope were all kept constant as far as possible. When both the dark-blue solution and colorless water are perfectly mixed, the standard deviation is equal to σ_{cm}. Thus, the mixing index is 100%. For a poor mixing case, the standard deviation is close to σ_{um} and the mixing index is near 0%. A value of X close to 100% represents a better mixing performance.

Figure 8 shows the mixing performance indicated by the mixing index. Among the three oscillating micromixers, the asymmetric micromixer with the splitter (AS-S) is clearly the best, the symmetric micromixer with the splitter (S-S) is good, and the symmetric micromixer without the splitter (S) is the worst, which agrees with the results of the flow patterns. A mixing index of 100% can be achieved in both the AS-S and the S-S, but the former with higher oscillating frequencies can more quickly reach the completed mixing than the latter with lower oscillating frequencies. In the S, the completed mixing cannot be achieved even at the largest Re of 386. Taking the S as an example, Figure 8 is divided into three regions according the flow patterns. As mentioned above, the recirculation mixing region features recirculation through the feedback channels, but the oscillation is not apparent. In the recirculation region, there is an upward trend for the mixing index. This is because the recirculation is enhanced by increasing Re, and consequently, the mixing performance is improved. It is obvious that the mixing performance is sufficiently enhanced within the oscillation mixing region compared with the two other regions. The largest mixing indexes are 57.0, 71.9, and 90.4% for the vortex, recirculation and oscillation mixing mechanisms, respectively. The oscillation mixing plays an important role in mixing the two miscible liquids.

To furthermore evaluate the mixing performance of the oscillating feedback micromixers, a sandwich micromixer and a Y-type micromixer were machined on a PMMA plate, respectively. Both the two micromixers are the lamination micromixer. The configuration of the sandwich micromixer and the Y-type micromixer are shown in Figures 9A

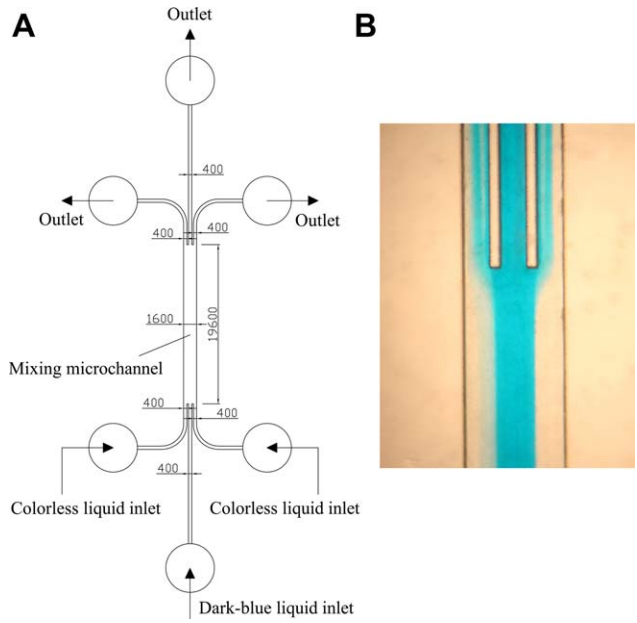

Figure 9. Sandwich micromixer: (A) configurations (Unit: micrometer), and (B) flow pattern near the outlet.

[Color figure can be viewed in the online issue, which is available at wileyonlinelibrary.com.]

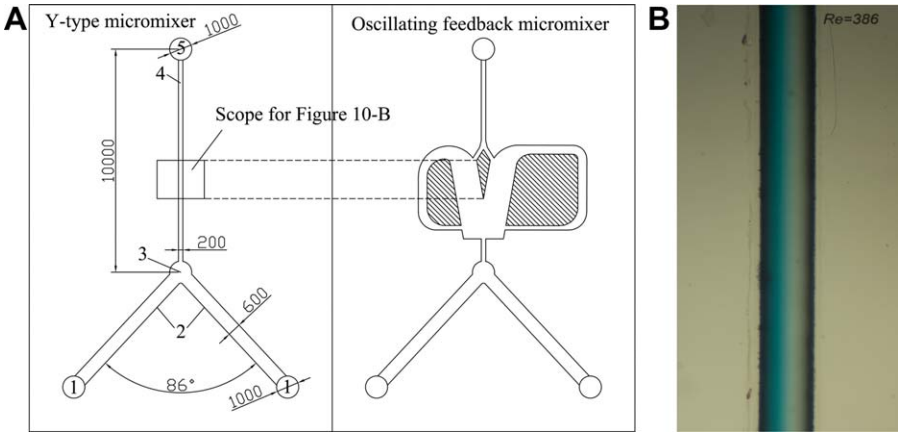

Figure 10. Y-type micromixer: (A) configurations (Unit: micrometer), and (B) flow pattern in the scope as shown in (A).

(1) Inlet port; (2) Y-feed channel; (3) Y-junction; (4) straight channel; and (5) outlet port. [Color figure can be viewed in the online issue, which is available at wileyonlinelibrary.com.]

and 10A, respectively. The dark-blue solution and colorless water identical to those used in the oscillating feedback micromixers were adopted. In the experiments for the sandwich micromixer, the dark-blue water was fed from the central inlet microchannel, while the colorless water was divided into the equivalent two parts and, respectively, fed from the outer inlet microchannels. The total volume rate of the colorless water is equal to the volume rate of the dark-blue water. Figure 9B is a picture near the outlet of the sandwich micromixer at an *Re* of 315.6. It can be seen that because of the hydraulic focusing effect, three lamellae are formed and almost no transverse flow occurs between adjacent lamellae. In the experiments for the Y-type micromixer, the dark-blue solution and the colorless water were fed separately from the two inlet ports and joined at the Y-junction. As shown in Figures 10A and 1, the Y-type micromixer has the same dimensions as the oscillating feedback micromixers, except for the two feedback channels and the mixing chamber. Namely, the Y-feed channel and the length from the Y-junction to the outlet port of the Y-type micromixer are both identical to those of the oscillating feedback micromixers. During the experiments, no significant mixing was observed in the experiments of the Y-type micromixer, even at the largest *Re* as shown in Figure 10B. Figure 8 gives a comparison among the Y-type micromixer and three oscillating feedback micromixers. The mixing indexes for the Y-type micromixer were determined using the same method as mentioned above. It is obvious that the Y-type micromixer has little mixing effect for Reynolds numbers in the range of 79–386, whereas the oscillating feedback micromixers have better mixing performance. Thus, transverse flows play a significant role to enhance mixing of two miscible liquids in a micromixer, and oscillating feedback micromixers can effectively improve mixing performance.

Conclusions

In this study, three oscillating feedback micromixers were experimentally investigated. There are three mixing mechanisms in oscillating feedback micromixers: vortex mixing, internal recirculation mixing, and oscillation mixing. The splitter and asymmetric feedback channels were shown to enhance the internal recirculation and oscillation. Efficient chaotic advection is achieved using oscillating feedback micromixers. The oscillating feedback micromixers are suitable for mixing different liquids with a high Reynolds number, and a mixing efficiency of 100% can be achieved for two miscible liquids.

Acknowledgment

This work was supported by the National Natural Science Foundation of China (No. 21276133).

Literature Cited

1. Hessel V, Löwe H, Schönfeld F. Micromixers—a review on passive and active mixing principles. *Chem Eng Sci*. 2005;60:2479–2501.
2. Nguyen NT, Wu Z. Micromixers—a review. *J Micromech Microeng*. 2005;15:R1–R16.
3. Gobby D, Angeli P, Gavrilidis A. Mixing characteristics of T-type microfluidic mixers. *J Micromech Microeng*. 2001;11:126–132.
4. Aoki N, Fukuda T, Maeda N, Mae K. Design of confluence and bend geometry for rapid mixing in microchannels. *Chem Eng J*. 2013;227:198–202.
5. Wu Z, Nguyen NT, Huang XY. Non-linear diffusive mixing in microchannels: theory and experiments. *J Micromech Microeng*. 2004;14:604–611.
6. Rosenfeld C, Serra C, Brochon C, Hadziioannou G. Influence of micromixer characteristics on polydispersity index of block copolymers synthesized in continuous flow microreactors. *Lab Chip*. 2008; 8:1682–1687.
7. Hessel V, Hardt S, Löwe H, Schönfeld F. Laminar mixing in different interdigital micromixers: I. experimental characterization. *AIChE J*. 2003;49:566–577.
8. Schönfeld F, Hessel V, Hofmann C. An optimized split-and –recombine micromixer with uniform 'chaotic' mixing. *Lab Chip*. 2004;4: 65–69.
9. Carrier O, Funfschilling D, Debas H, Poncin S, Löb P, Li HZ. Pressure drop in a split-and-recombine caterpillar micromixer in case of newtonian and non-newtonian fluids. *AIChE J*. 2013;59(7): 2679–2685.
10. Kockmann N, Foll C, Woias P. Flow regimes and mass transfer characteristics in static micromixers. *Proc SPIE*. 2003;4982: 319–329.
11. Dreher S, Kockmann N, Woias P. Characterization of laminar transient flow regimes and mixing in T-shaped micromixers. *Heat Transfer Eng*. 2009;30(1–2):91–100.
12. Orsi G, Galletti C, Brunazzi E, Mauri R. Mixing of two miscible liquids in T-shaped microdevices. *Chem Eng Trans*. 2013;32: 1471–1476.
13. Paik P, Pamula VK, Fair RB. Rapid droplet mixers for digital microfluidic systems. *Lab Chip*. 2003;3:253–259.

14. Yang BD, Lu YC, Luo GS. Controllable preparation of polyacrylamide hydrogel microspheres in a coaxial microfluidic device. *Ind Eng Chem Res*. 2012;51:9016–9022.
15. Song H, Bringer MR, Tice JD, Gerdts CJ, Ismagilov RF. Experimental test of scaling of mixing by chaotic advection in droplets moving through microfluidic channels. *Appl Phys Lett*. 2003;83:4664–4666.
16. Su YH, Chen GW, Yuan Q. Influence of hydrodynamics on liquid mixing during Taylor flow in a microchannel. *AIChE J*. 2012;58(6):1660–1670.
17. Aref H. Stirring by chaotic advection, *J Fluid Mech*. 1984;143:1–21.
18. Ottino JM. *The Kinematics of Mixing: Stretching, Chaos, and Transport*. New York: Cambridge University Press, 1989.
19. Stroock AD, Dertinger SKW, Ajdari A, Mezić I, Stone HA, Whitesides GW. Chaotic mixer for microchanels. *Science* 2002;295:647–651.
20. Jang F, Drese KS, Hardt S, Küpper M, Schönfeld F. Helical flows and chaotic mixing in curved microchannels. *AIChE J*. 2004;50:2297–2305.
21. Hong CC, Choi JW, Ahn CH. A novel in-plane microfluidic mixer with modified Tesla structures. *Lab Chip*. 2004;4:109–113.
22. Mizuno Y, Funakoshi M. Chaotic mixing due to a spatially periodic three-dimensional flow. *Fluid Dyn Res*. 2002;31:129–149.
23. Mengeaud V, Josserand J, Girault HH. Mixing processes in a zigzag microchannel: finite element simulation and optical study. *Anal Chem*. 2002;74:4279–4286.
24. Kim DS, Lee SW, Kwon TH, Lee SS. A barrier embedded chaotic micromixer. *J Micromech Microeng*. 2004;14:798–805.
25. Lee CY, Chang CL, Wang YN, Fu LM. Microfluidic mixing: a review. *Int J Mol Sci*. 2011;12:3263–3287.
26. Cook KJ, Fan YF, Hassan I. Mixing evaluation of a passive scaled-up serpentine micromixer with slanted grooves. *J Fluids Eng*. 2013;135:1–12.
27. Hsiao KY, Wu CY, Huang YT. Fluid mixing in a microchannel with longitudinal vortex generators. *Chem Eng J*. 2014;235:27–36.
28. La M, Park SJ, Kim HW, Park JJ, Ahn KT, Ryew SM, Kim DS. A centrifugal force-based serpentine micromixer (CSM) on a plastic lab-on-a-disk for biochemical assays. *Microfluid Nanofluidic*. 2013;15:87–98.
29. Kuo JN, Jiang LR. Design optimization of micromixer with square-wave microchannel on compact disk microfluidic platform. *Microsyst Technol*. 2014;20:91–99.
30. Garofalo F, Adrover A, Cerbelli S, Giona M. Spectral characterization of static mixers: the S-shaped micromixer as a case study. *AIChE J*. 2010;56(2):318–335.
31. Yun SC, Lim G, Kang KH, Suh YK. Geometric effects on lateral transport induced by slanted grooves in a microchannel at a low Reynolds number. *Chem Eng Sci*. 2013;104:82–92.
32. Jen CP, Wu CY, Lin YC, Wu CY. Design and simulation of the micromixer with chaotic advection in microchannels. *Lab Chip*. 2003;3:77–81.
33. Kirshner JM, Katz S. *Design Theory of Fluidic Components*. London: Academic Press, 1975.
34. Tippetts JR, Ng HK, Royle JK. Oscillating bistable fluid amplifier for use as a flowmeter. *Fluidics Q*. 1973;5:28–42.
35. Yamasaki H. Progress in hydrodynamic oscillator type flowmeters. *Flow Meas Instrum*. 1993;4(4):241–247.
36. Yang JT, Chen CK, Tsai KJ, Lin WZ, Sheen HJ. A novel fluidic oscillator incorporating step-shaped attachment walls. *Sens Actuators A Phys*. 2007;135:476–483.
37. Xu C, Meng XD, Yu H. Performance characteristic curve insensitive to feedback fluidic oscillator configurations. *Sens Actuators A Phys*. 2013;189:55–60.
38. Wang J, Xu C. Mini liquid-liquid extractor without moving parts based on the Coanda effect, *Chem Eng Technol*. 2014;37(3):535–542.
39. Yang JT, Chen CK, Hu IC, Lyu PC. Design of a self-flapping microfluidic oscillator and diagnosis with fluorescence methods, *J Microelectromech Syst*. 2007;16(4):826–835.

Manuscript received May 19, 2014, and revision received Nov. 3, 2014.